受入
84-10-191
高工研図書室

EUROPEAN ORGANIZATION FOR NUCLEAR RESEARCH

CERN-EP/84-99
8 August 1984

# A NEW MEASUREMENT OF THE RATIO OF THE CROSS-SECTIONS OF MUON-NEUTRINO AND MUON-ANTINEUTRINO SCATTERING ON ELECTRONS

CHARM Collaboration

F. Bergsma and J. Dorenbosch
NIKHEF, Amsterdam, The Netherlands

J. V. Allaby, U. Amaldi, G. Barbiellini[*)], M. Baubillier, C. Busi,
W. Flegel, F. Grancagnolo, L. Lanceri, M. Metcalf, C. Nieuwenhuis,
J. Panman, R. Plunkett, C. Santoni[**)] and K. Winter
CERN, Geneva, Switzerland

I. Abt, J. Aspiazu, F. W. Büsser, H. Daumann, P. D. Gall, T. Hebbeker,
F. Niebergall, P. Schütt and P. Stähelin
II. Institut für Experimentalphysik[***)], Universität Hamburg,
Hamburg, Fed. Rep. Germany

P. Gorbunov, E. Grigoriev, V. Kaftanov, V. Khovansky and A. Rosanov
Institute for Theoretical and Experimental Physics, Moscow, USSR

A. Baroncelli[+)], L. Barone[++)], B. Borgia[++)], C. Bosio[+)], A. Capone[++)],
M. Diemoz[++)], U. Dore[++)], F. Ferroni[++)], E. Longo[++)], L. Luminari[++)],
P. Monacelli[++)], S. Morganti[+++)], F. de Notaristefani[++)],
L. Tortora[+)] and V. Valente[+++)]
Istituto Nazionale di Fisica Nucleare, Roma, Italy

(Submitted to Physics Letters)

---

*) On leave of absence from Laboratori Nazionali dell'INFN, Frascati, Italy.

**) On leave of absence from INFN Sezione Sanità and Istituto Superiore di Sanità, Roma, Italy.

***) Supported by Bundesministerium für Forschung und Technologie, Bonn, German Federal Republic.

+) INFN Sezione Sanità and Istituto Superiore di Sanità, Roma, Italy.

++) Istituto di Fisica, University of Roma and INFN Sezione di Roma, Italy.

+++) Laboratori Nazionali dell'INFN, Frascati, Italy.

ABSTRACT

A new experimental determination of the electro-weak mixing angle $\theta_W$ is reported based on a second exposure of the CHARM calorimeter to the CERN SPS wide-band beam. The ratio R of muon-neutrino and muon-antineutrino electron scattering cross-sections has been determined from a sample of 37 ± 10 and 35 ± 10 events. The experimental result is R = 1.26 + 0.72/- 0.45, corresponding to a value of $\sin^2 \theta_W = 0.216 \pm 0.055$. The total sample of events collected in the CHARM calorimeter during the two exposures is (83 ± 16) $\nu_\mu e$ events and (112 ± 21) $\bar{\nu}_\mu e$ events, leading to the final result $\sin^2 \theta_W = 0.215 \pm 0.032$. The systematic error is estimated to be ± 0.012.

According to the standard model, the ratio R of the cross-sections for muon-neutrino and muon-antineutrino scattering on electrons is a function of the electro-weak mixing angle $\theta_W$ [1]:

$$R = \frac{\sigma(\nu_\mu e)}{\sigma(\bar{\nu}_\mu e)} = 3 \times \frac{1 - 4 \sin^2 \theta_W + (16/3) \sin^4 \theta_W}{1 - 4 \sin^2 \theta_W + 16 \sin^4 \theta_W} \quad . \qquad (1)$$

A measurement of R, obtained in a first exposure of the CHARM detector [2], has been reported previously [3]. The error on the value of $\sin^2 \theta_W$ obtained was largely dominated by statistical uncertainty. A new exposure of the fine-grain CHARM detector [2] to the horn-focused wide band neutrino beam of the CERN 400 GeV Super Proton Synchrotron (SPS) has therefore been performed.

Since the earlier measurements the CHARM calorimeter has been refined by the addition of planes of limited streamer tubes [4] and by an increased dynamical range (3×) of the pulse-height measurement in the proportional drift tubes [5] to improve the angular resolution of electromagnetic showers. It is described in detail in ref. [5], where the results obtained on the calibration of the detector in electron and pion test beams are also reported. The angular resolution of electron showers was improved by a factor of about ≈1.4 (at 15 GeV, for example, it went from 16 to 11 mrad), mainly because of a better vertex reconstruction, achieved with the aid of both streamer and proportional drift tube systems. The other characteristics of the improved CHARM detector are briefly recalled here. It consists of 78 subunits, each one including a marble plate of 300 × 300 $cm^2$ surface area and 8 cm thickness (≈ 1 radiation length) followed by three planes of sensitive elements: i) a plane of 128 proportional drift tubes (3 × 3 × 400 $cm^3$), ii) a plane of 20 plastic scintillation counters (15 × 3 × 300 $cm^3$) oriented perpendicularly with respect to the direction of the proportional drift tubes, and iii) a plane of 256 limited streamer tubes (1 × 1 × 265 $cm^3$) oriented along the scintillators. During this exposure the first 6 modules have been moved to the side to search for decays of penetrating neutral particles produced by the interaction of protons in the target. The target calorimeter is followed by the muon spectrometer made of segmented toroidal iron magnets interspersed with 18 planes of proportional drift tubes and 6 planes of scintillation counters [2].

The detector was exposed to neutrino and antineutrino beams for an integrated flux of $1.2 \times 10^{18}$ and $2.3 \times 10^{18}$ protons on target, respectively. A total number of $1.2 \times 10^{6}$ ($7.6 \times 10^{5}$) neutrino (antineutrino) interactions was recorded in the calorimeter.

The cross-section for (anti)neutrino electron scattering is expected to be three to four orders of magnitude smaller than the (anti)neutrino nucleon cross-section at the same neutrino energy. A clear separation of these event types is therefore required. Events with a single recoiling electron were identified by the different behaviour of electromagnetic and hadronic showers in the CHARM detector [5] and by the distinctive characteristics of the kinematics of the $\overset{(-)}{\nu}_{\mu}e$ scattering interactions as compared with those of semileptonic processes.

The events were first filtered using a simple and fast algorithm that required: i) less than 4 of the 6 scintillator planes in the muon spectrometer hit to reject charged-current $\overset{(-)}{\nu}_{\mu}$ induced events with ≈70% geometrical efficiency, without loss of electron candidates and ii) a streamer tube hit pattern with a limited number of gaps in the lateral shower profiles observed in the first 8 planes of the shower. This criterion was derived from an extensive study of the hit density of the showers produced by electrons and pions in a test beam [5]. Events were passed to the final analysis step if the interaction occurred in the fiducial volume of $230 \times 230$ cm$^2$ in transverse area and in the first 57 subunits in length, and if the shower energy E was between 4 and 30 GeV. The increase in energy acceptance (the lower limit was 7.5 GeV in the analysis of the data of the previous exposure [3]) corresponds to an increase in statistics of approximately 30%.

Criteria based on the shower properties were used for each of the three planes of sensitive elements following the vertex: i) the energy $E_F$ deposited in the first scintillator plane was required to be $E_F < 50$ MeV, corresponding to less than 7 minimum ionizing particles, ii) only one proportional drift tube must be hit in the first plane, and iii) in the first streamer tube plane a maximum of 6 hits with no more than 2 gaps were allowed. Criteria i) and ii) were also used in the previous analysis [3].

Two additional parameters, describing the transverse shape of the showers, were introduced in order to distinguish between electromagnetic and hadronic showers: the width, $\Gamma$, of the distribution of the energy-deposited in the scintillators and the root mean square, $\sigma_{ST}$, of the distribution of the hits in the streamer tubes, both projected in a plane perpendicular to the shower axis. They are sensitive to different properties of the showers. The first one is related to the energy deposition density in the core of the shower, because of the linear response of the scintillators. The second one is more sensitive to the tail of the shower, given the digital readout of the limited streamer tubes. Suitable cuts on $\Gamma$ and $\sigma_{ST}$ were chosen in order to reject hadronic showers by a factor of approximately 100 and to get a global efficiency of approximately 85% when applied to electron test beam data.

The $E^2\theta^2$ distributions, where $\theta$ is the shower angle with respect to the neutrino beam axis, for the events satisfying the selection criteria, are shown in figs. 1a and b. The number of $\overset{(-)}{\nu}_\mu e$ candidates with $E^2\theta^2 < 0.54$ GeV$^2$ is 339 (376). The bulk of the $\overset{(-)}{\nu}_\mu e$ signal (87%), according to the measured angular resolution, is expected in the interval $E^2\theta^2 < 0.06$ GeV$^2$ (forward region). Neutrino electron scattering events were obtained by subtracting, in the forward region, the background measured in the reference region ($0.12 < E^2\theta^2 < 0.54$ GeV$^2$) and extrapolated according to the hypothesis of a two-component background [3]: a) quasi-elastic charged-current events on nucleons induced by the $\overset{(-)}{\nu}_e$ contamination of the beam, b) neutral-current events with a $\gamma$ and/or a $\pi^0$ in the final state produced by coherent scattering of $\overset{(-)}{\nu}_\mu$ on nuclei. The relative amount of the two backgrounds was evaluated, as in ref. [3], from the study of the $E_F$ distribution, which is different for showers initiated by electrons or by $\pi^0$'s and $\gamma$'s. Since the $E^2\theta^2$ distributions of the two backgrounds are quite similar, a possible error in the composition of the total background has little effect on the number of the $\nu_\mu e$ and $\bar{\nu}_\mu e$ events. The results of this analysis are summarized in table 1. The number of events due to the signal is found to be $37 \pm 10$ and $35 \pm 10$ for the $\nu$ and $\bar{\nu}$ beams, respectively. Taking into account the improved angular resolution and the differences of the acceptance criteria, the signal-to-background ratio and the background composition agree within the statistical errors with the results presented in ref. [3]. Consistent results for the background subtraction have been obtained by applying a maximum-likelihood criterion to the distribution of the events in the plane E-$\theta$.

The (anti)neutrino beam flux was monitored by recording the events induced by quasi-elastic charged-current processes on nucleons [6]:

$$\overset{(-)}{\nu}_\mu \, N \rightarrow \mu^{\pm} \, N' \tag{2}$$

and the events induced by inclusive charged-current and neutral-current processes on nucleons [7]:

$$\overset{(-)}{\nu}_\mu N \rightarrow \mu^\pm X$$

$$\overset{(-)}{\nu}_\mu N \rightarrow \overset{(-)}{\nu}_\mu X \qquad (3)$$

The charge of the muons produced in reaction (2) gave information on the relative contamination due to the wrong type of muon neutrino component in the beams. The $\overset{(-)}{\nu}_e$ contamination was computed by a Monte Carlo simulation [8] tuned to obtain the measured rates of $\overset{(-)}{\nu}_\mu$ events. The following energy-weighted ratios of the components of the neutrino and antineutrino beams were, respectively, obtained:

$$\nu_\mu : \bar{\nu}_\mu : \nu_e : \bar{\nu}_e = 1 : 0.06 : 0.017 : 0.004$$

$$\bar{\nu}_\mu : \nu_\mu : \bar{\nu}_e : \nu_e = 1 : 0.10 : 0.012 : 0.006 \qquad (4)$$

The uncertainty is negligible for the wrong-sign muon-neutrino components and is 50% for the electron-neutrino components.

Applying corrections for the presence of neutrinos of the wrong kind in the two beams, the number of events attributed to $\nu_\mu e$ and $\bar{\nu}_\mu e$ scattering becomes $N(\nu_\mu e) = 33 \pm 10$ and $N(\bar{\nu}_\mu e) = 31 \pm 10$, respectively. The corrections depend only slightly on $\sin^2 \theta_W$, for which a value of 0.22 was assumed.

The value of R was obtained from the ratio of the events normalized to the energy-weighted fluxes. The normalization factor was computed using the number of the events induced by reactions (2) and (3) collected in the detector during the exposure. In the first case, since the quasi-elastic processes (2) in the interval $0.05 < Q^2 < 0.2$ GeV$^2$ have cross-sections which are almost energy independent at neutrino energies larger than 4 GeV and nearly equal for $\nu$ and $\bar{\nu}$ (a correction for the small difference was applied), the ratio of the energy-weighted fluxes is given by

$$F_Q = \frac{N_Q(\bar{\nu}) \ \langle E_{\bar{\nu}} \rangle}{N_Q(\nu) \ \langle E_\nu \rangle} = 1.25 \pm 0.08 \quad , \qquad (5)$$

where $N_Q(\nu)$ are the observed numbers of events and $\langle E_\nu \rangle$ the mean value of the energy of the muon-neutrino beam obtained by unfolding the measured energy distribution of the events. $\langle E_\nu \rangle$ is found to be 26 GeV for neutrinos and 21 GeV for antineutrinos. The inclusive processes (3) have a cross-section rising linearly with energy, and the ratio of the energy-weighted fluxes is given by

$$F_I = \frac{N_I(\bar{\nu})\ \sigma_0(\nu)}{N_I(\nu)\ \sigma_0(\bar{\nu})} = 1.12 \pm 0.08 \quad , \qquad (6)$$

where $N_I(\nu)$ are the observed numbers of events and $\sigma_0(\nu)$ the cross-section slopes for deep inelastic scattering [7] of neutrinos and antineutrinos. By taking the average of $F_I$ and $F_Q$ a value of $F = 1.18 \pm 0.06$ was obtained.

The ratio of the normalized number of $\nu_\mu e$ and $\bar{\nu}_\mu e$ events is

$$R_{exp} = \frac{N(\nu_\mu e)}{N(\bar{\nu}_\mu e)} \times F = 1.26\ {}^{+0.72}_{-0.45}\ (\mathrm{stat}) \quad . \qquad (7)$$

The measured quantity $R_{exp}$ agrees with the predictions of the standard model for

$$\sin^2 \theta_W = 0.216 \pm 0.055\ (\mathrm{stat}) \pm 0.010\ (\mathrm{syst}) \ , \qquad (8)$$

as shown in fig. 2. The solid curve represents the expected ratio between the fraction of neutrino and antineutrino cross-sections which satisfy the requirement imposed on the recoil electron energy in the analysis (4 GeV $< E <$ 30 GeV). The effect of the energy cuts on R is negligible as is evident by comparing the solid curve with the expectation of R for full energy acceptance (dashed curve). The main systematic errors on R are due to the background subtraction (± 7%) and to the normalization (± 5%) uncertainties; added quadratically, they lead to the systematic uncertainty of ± 0.010 on $\sin^2 \theta_W$ [see eq. (8)].

To evaluate the neutrino and antineutrino cross-sections, the global efficiency of the criteria applied to separate showers induced by single electrons was determined experimentally from the electron test data [5]. It is weakly energy dependent and the mean value, folded with the predicted energy distribution is (58 ± 5)%, equal for the neutrino and antineutrino events. By using the procedure outlined in ref. [9], the following cross-sections are obtained:

$$\frac{\sigma(\nu_\mu e)}{E_\nu} = [1.8 \pm 0.5\ (\text{stat}) \pm 0.4\ (\text{syst})] \times 10^{-42}\ \text{cm}^2/\text{GeV}$$

$$\frac{\sigma(\bar{\nu}_\mu e)}{E_{\bar{\nu}}} = [1.4 \pm 0.5\ (\text{stat}) \pm 0.4\ (\text{syst})] \times 10^{-42}\ \text{cm}^2/\text{GeV}\ , \qquad (9)$$

in good agreement with our previous measurements [3,9].

The ratio of the neutral-current and charged-current coupling strengths, as determined from the simultaneous measurements of R and $\sigma(\overset{(-)}{\nu}_\mu e)$, is

$$\rho = 1.05 \pm 0.13\ (\text{stat}) \pm 0.10\ (\text{syst}) \quad . \qquad (10)$$

The $E^2\theta^2$ distributions of all $\nu_\mu e$ and $\bar{\nu}_\mu e$ candidate events collected in the old and in the new exposure of the CHARM detector are shown in figs. 3a and b which take into account the different angular resolutions. Figures 3c and d show the analogous distributions for events satisfying the additional condition $E_F < 8$ MeV, in order to select unambiguously those events with a single electron at the shower vertex. After the background subtraction, the following numbers of $\overset{(-)}{\nu}_\mu e$ events, contained in the first bin of figs. 3a and b are found: 83 ± 16 and 112 ± 21, respectively. From the $E^2\theta^2$ distributions of the events with $E_F < 8$ MeV (figs. 3c and d) signals of 24 ± 6 and 35 ± 9 events were obtained from the neutrino and antineutrino exposures, respectively. The ratio of the signals found with $E_F < 8$ MeV and with $E_F < 50$ MeV is 0.30 ± 0.08, in very good agreement with the relative selection efficiency of 0.32 ± 0.05, as measured in the electron test beam. This agreement supports the hypothesis that the signals are due to events with a single recoil electron.

Combining the results of the two exposures, the following results were obtained:

$$\sin^2\theta_W = 0.215 \pm 0.032\ \text{(stat)} \pm 0.012\ \text{(syst)}$$

$$\frac{\sigma(\nu_\mu e)}{E_\nu} = [1.9 \pm 0.4\ \text{(stat)} \pm 0.4\ \text{(syst)}] \times 10^{-42}\ \text{cm}^2/\text{GeV}$$

$$\frac{\sigma(\bar{\nu}_\mu e)}{E_{\bar{\nu}}} = [1.5 \pm 0.3\ \text{(stat)} \pm 0.4\ \text{(syst)}] \times 10^{-42}\ \text{cm}^2/\text{GeV} \qquad (11)$$

$$\rho = 1.09 \pm 0.09\ \text{(stat)} \pm 0.11\ \text{(syst)} \quad .$$

In summary, the new exposure of the improved CHARM calorimeter to the SPS wide-band neutrino beam has led to a reduced statistical error (15%) on the measurement of $\sin^2\theta_W$ in purely leptonic interactions, and to a smaller systematic error.

Four values of neutral-current coupling constants $g_A^e$ and $g_V^e$ can be obtained from the measurements of R and $\sigma(\overset{(-)}{\nu}_\mu e)$, as shown in fig. 4. The limits from other measurements in the lepton sector (fig. 4), those from the forward-backward asymmetry in the reaction $e^+e^-\to l^+l^-$ at PETRA [10] and from $\bar{\nu}_e e$ scattering cross-section [11] (evaluated in ref. [12]), select a unique solution:

$$g_A^e = -0.54 \pm 0.05\ \text{(stat)} \pm 0.06\ \text{(syst)}$$

$$g_V^e = -0.08 \pm 0.07\ \text{(stat)} \pm 0.03\ \text{(syst)} \qquad (12)$$

A value of $g_A^e=-1/2$ is predicted by the standard model [1], in agreement with the experiment.

Acknowledgements

We wish to thank E. Iarocci and his group for acquainting us with the technique of streamer tubes. We would like to express our gratitude and appreciation to our numerous technical collaborators who contributed to the recent improvements of the CHARM detector. The successful implementation of these improvements was possible thanks to their skill and dedication. In particular, we would like to thank W. Albrecht and his group for technical help; G. Basti, R. Donnet, E. Gygi, M. Jimenez, A. King, F. Schneider and P. Veneroni for the design and the construction of the streamer tubes; and R. Dupuis, M. Ferrat, B. Friend, G. W. Gotink, H. L. Groenstege, S. Guerra, D. De Pedis and J. Schütt for the design and construction of the electronics of the streamer tubes and the proportional drift tubes. J. Audier has helped with the data handling. We also wish to express our gratitude to G. Cocconi, A. N. Diddens, M. Jonker, F. Udo and A. M. Wetherell for their contributions to this experiment.

## REFERENCES


1. S. L. Glashow, Nucl. Phys. 22 (1961) 579.
   S. Weinberg, Phys. Rev. Lett. 19 (1967) 1264.
   A. Salam, Elementary Particle Theory (ed. N. Svartholm) (Almqvist and Wiksell, Stockholm, 1968), p. 367.
   G. W.'t Hooft, Phys. Lett. 37B (1971) 195.

2. A. N. Diddens et al. (CHARM Collab.), Nucl. Instrum. Methods 178 (1980) 27.
   M. Jonker et al. (CHARM Collab.), Nucl. Instrum. Methods 200 (1982) 183.

3. M. Jonker et al. ( CHARM Collab.), Phys. Lett. 117B (1982) 272.

4. M. Jonker et al., Nucl. Instrum. Methods 215 (1983) 361.

5. F. Bergsma et al. (CHARM Collab.), to be submitted to Nucl. Instrum. Methods.

6. M. Jonker et al. (CHARM Collab.), Phys. Lett. 93B (1980) 203.
   F. Bergsma et al. (CHARM Collab.), Phys. Lett. 122B (1983) 465.

7. M. Jonker et al. (CHARM Collab.), Phys. Lett. 99B (1981) 261.

8. C. Visser, NUBEAM, CERN HYDRA Application Library (1979).

9. M. Jonker et al. (CHARM Collab.), Phys. Lett. 105B (1981) 242.

10. J. Panman, Rapporteur's talk, Proc. Neutrino '84, Dortmund, 1984, to be published.

11. F. Reines, H. S. Gurr and H. W. Sobel, Phys. Rev. Lett. 37 (1976) 315.

12. W. Krenz, RWTH Aachen preprint, Pitha 82/26 (1982).

## Table 1

"Signal" and "background" in the forward and reference regions

| Beam | $\nu$ | $\bar{\nu}$ |
|---|---|---|
| Reference region $0.12 < E^2\theta^2 < 0.54$ GeV$^2$ | | |
| Background, electron-induced (a) | 77 ± 17 | 88 ± 19 |
| photon-induced (b) | 133 ± 22 | 141 ± 24 |
| Forward region $E^2\theta^2 < 0.06$ GeV$^2$ | | |
| Background, electron-induced (a) | 22 ± 5 | 25 ± 5 |
| photon-induced (b) | 26 ± 4 | 28 ± 5 |
| Bulk of $\overset{(-)}{\nu}_\mu e$ signal (87%) | 37 ± 10 | 35 ± 10 |

Figure Captions

Fig. 1 $E^2\theta^2$ distributions for a) neutrino and b) antineutrino events selected by the criteria discussed in the text. The backgrounds of $\overset{(-)}{\nu}_e$ induced charged-current (CC) events and $\overset{(-)}{\nu}_\mu$ induced neutral-current (NC) events, shown in the figures, are summarized in table 1.

Fig. 2 Ratio of muon-neutrino electron to muon-antineutrino electron cross sections as a function of $\sin^2\theta_W$ . The full curve represents the expectation for events in the electron energy range 4 to 30 GeV. The dashed curve represents the expectation in the case of full energy acceptance. The measured value of R and its statistical error are shown together with the corresponding values for $\sin^2\theta_W$ .

Fig. 3 $E^2\theta^2$ distributions for a) neutrino and b) antineutrino events collected in the old and in the new exposure. The new data are shown using a horizontal scale expanded by a factor of 2 in order to take into account the different angular resolution ($\Delta\theta^2_{old} \approx 2\ \Delta\theta^2_{new}$). The same scale correction has been applied in the computation of the two backgrounds. Figures. 3c and d show the analogous distributions for the events satisfying the additional condition that the energy deposited by the showers in the first scintillator plane be $E_F < 8$ MeV. In this case the background is due only to $\overset{(-)}{\nu}_e$ quasi-elastic scattering.

Fig. 4 Values of neutral-current coupling constants of the electron, $g_V^e$, $g_A^e$, obtained from the measurement of R and of the $\nu_\mu e$ and $\bar{\nu}_\mu e$ cross-sections. The statistical and systematic errors are combined in quadrature. The limits from the measurements of the forward-backward asymmetry in the reaction $e^+e^-\rightarrow l^+l^-$ at PETRA and PEP [10] and of $\bar{\nu}_e e$ scattering cross-section [11, 12] select a unique solution.

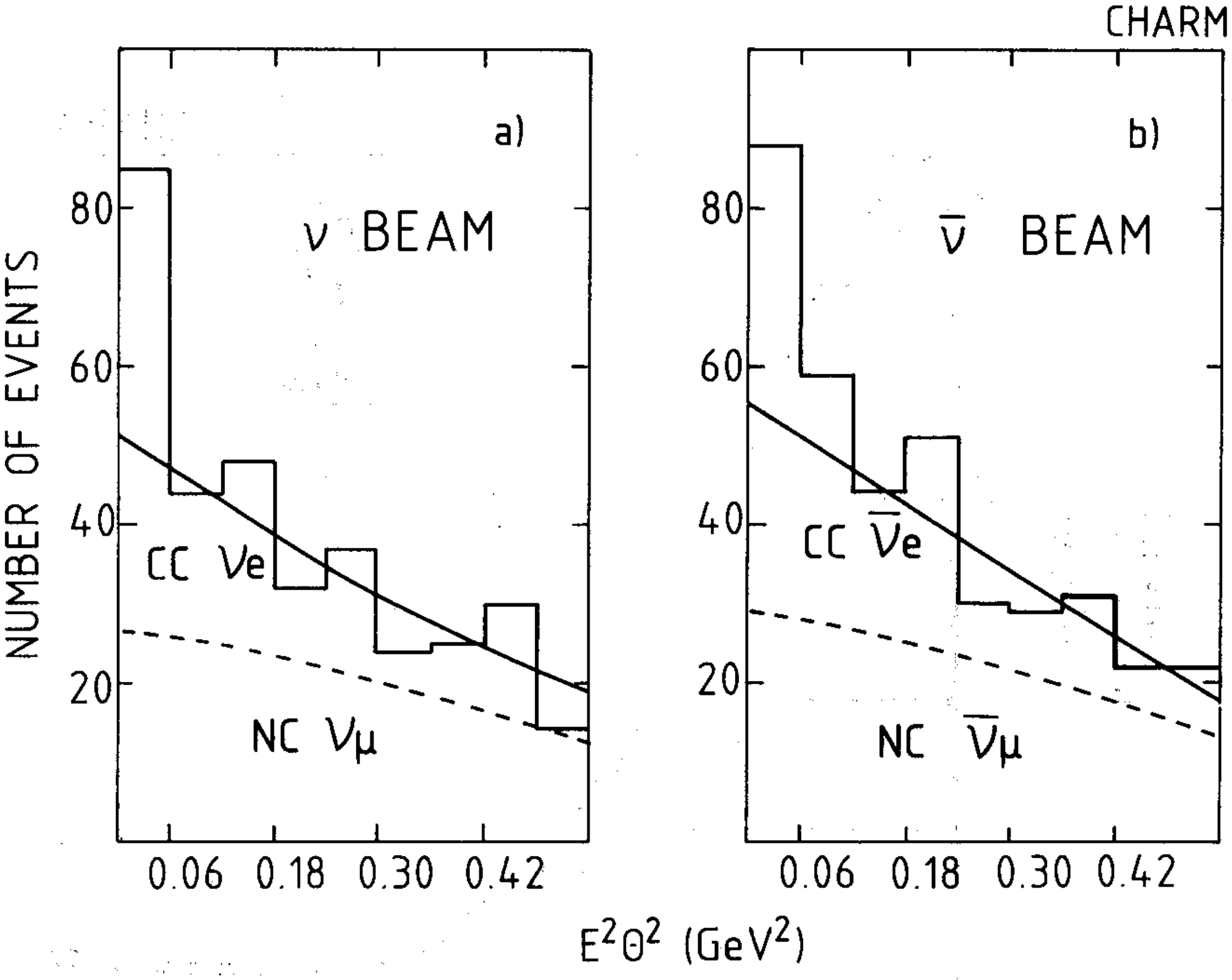
CHARM
a)
ν BEAM
CC νe
NC νμ
b)
ν̄ BEAM
CC ν̄e
NC ν̄μ
NUMBER OF EVENTS
80
60
40
20
0.06
0.18
0.30
0.42
E²Θ² (GeV²)

Fig. 1

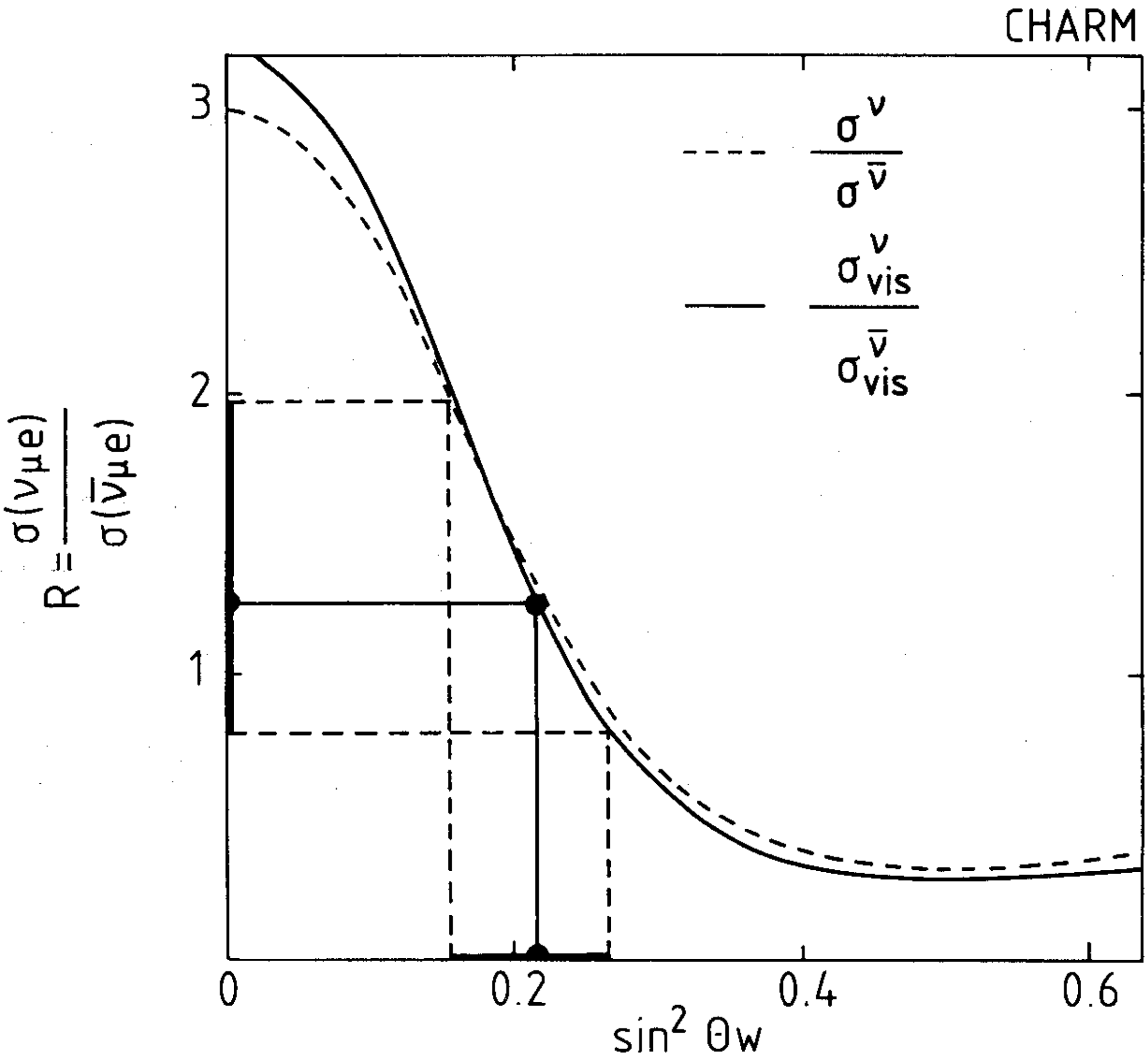
CHARM
3
2
1
0
0.2
0.4
0.6
$\sin^2 \Theta w$
$R = \frac{\sigma(\nu_\mu e)}{\sigma(\bar{\nu}_\mu e)}$
$\frac{\sigma^\nu}{\sigma^{\bar{\nu}}}$
$\frac{\sigma^\nu_{vis}}{\sigma^{\bar{\nu}}_{vis}}$

Fig. 2

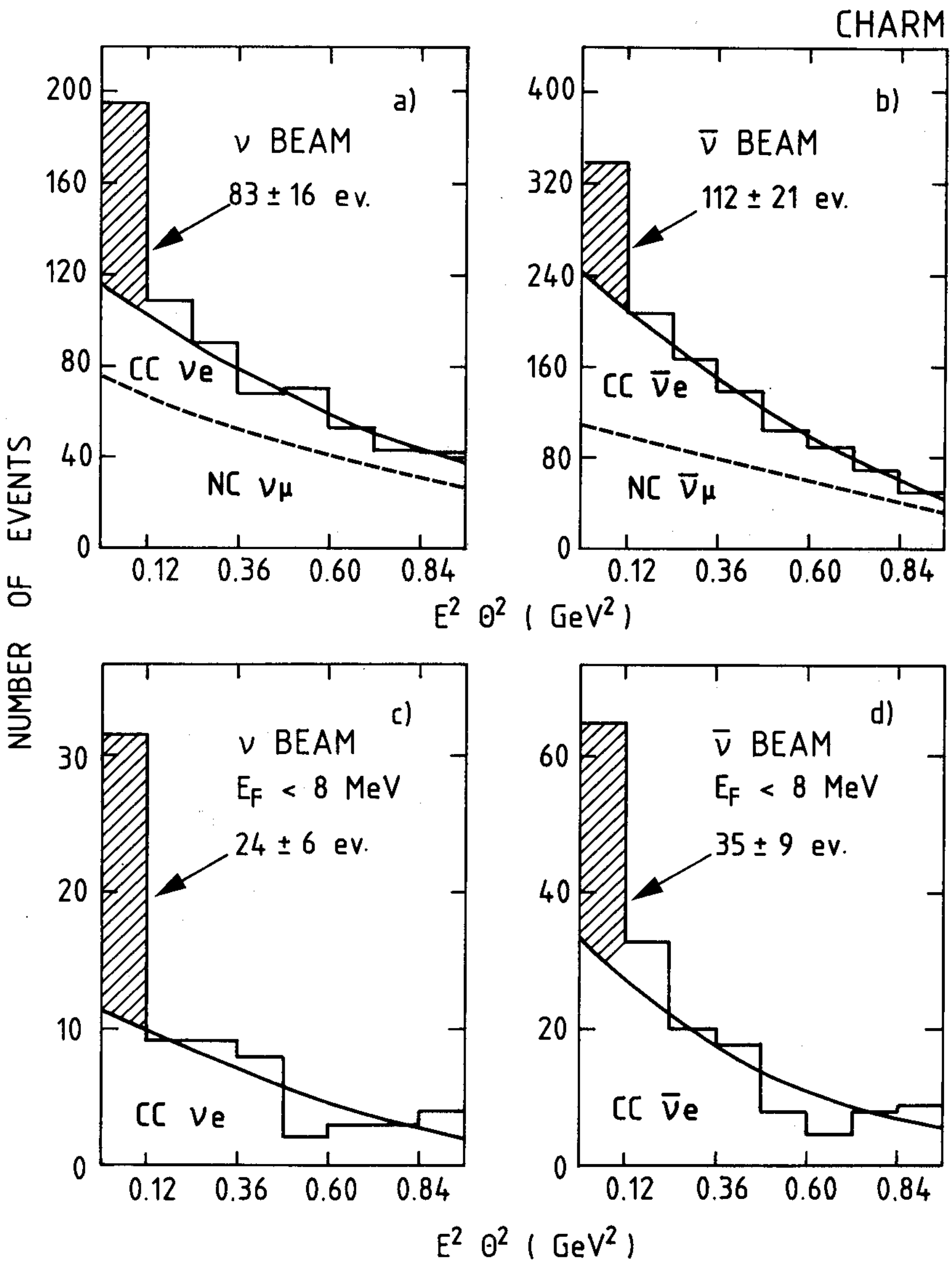

CHARM
a)
ν BEAM
83 ± 16 ev.
CC νe
NC νμ
b)
ν̄ BEAM
112 ± 21 ev.
CC ν̄e
NC ν̄μ
c)
ν BEAM
E_F < 8 MeV
24 ± 6 ev.
CC νe
d)
ν̄ BEAM
E_F < 8 MeV
35 ± 9 ev.
CC ν̄e
NUMBER OF EVENTS
E² θ² ( GeV² )


Fig. 3

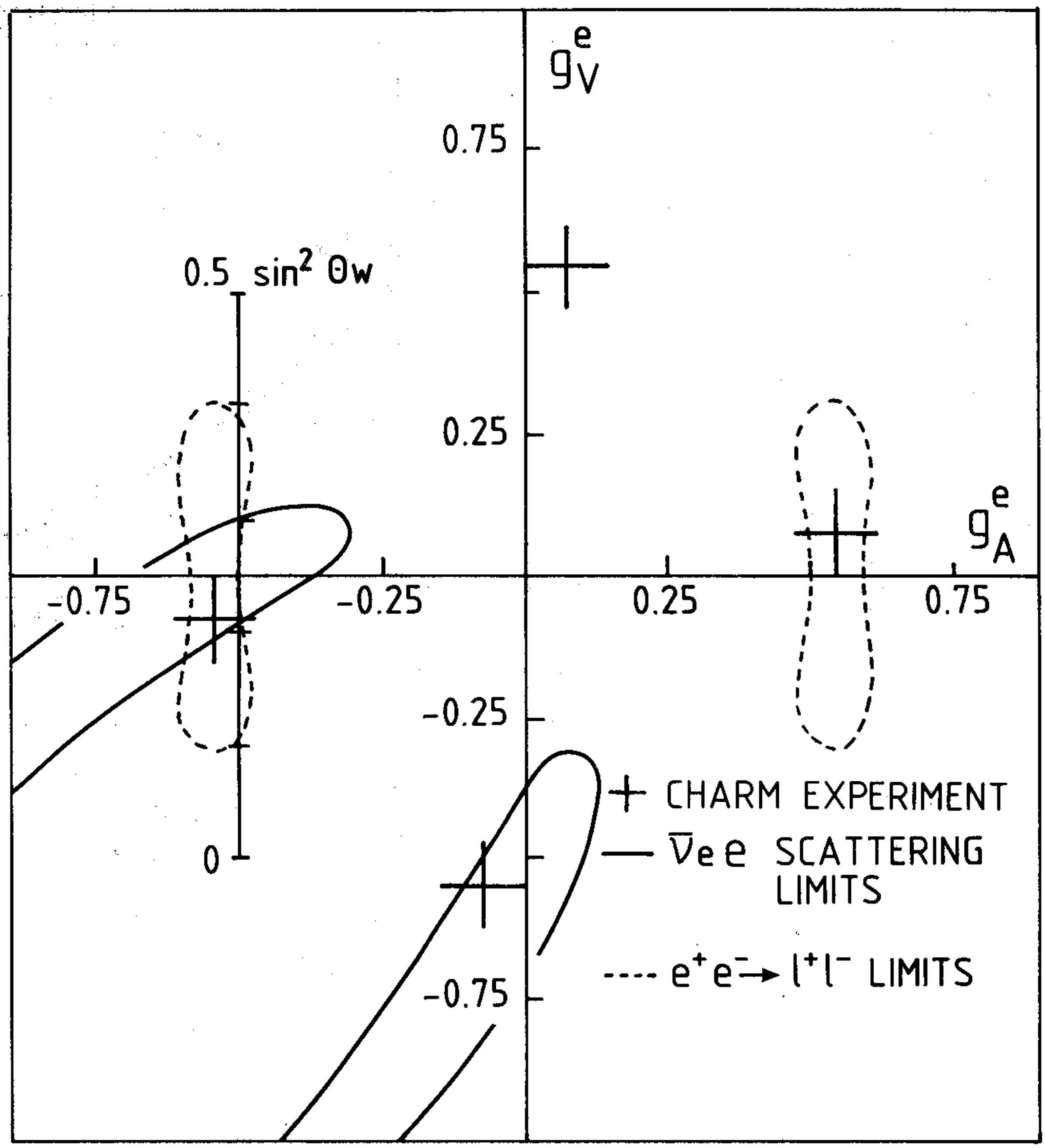

$g_V^e$
0.75
0.5 $\sin^2\Theta w$
0.25
$g_A^e$
-0.75
-0.25
0.25
0.75
-0.25
0
-0.75
CHARM EXPERIMENT
$\bar{\nu}_e e$ SCATTERING LIMITS
$e^+e^- \rightarrow l^+l^-$ LIMITS


Fig. 4